2021

Green underwater wireless communications using hybrid optical-acoustic technologies

Kazi Y. Islam

Iftekhar Ahmad

Daryoush Habibi

M. Ishtiaque A. Zahed

Joarder Kamruzzaman

10.1109/ACCESS.2021.3088467 Islam, K. Y., Ahmad, I., Habibi, D., Zahed, M. I. A., & Kamruzzaman, J. (2021). Green underwater wireless communications using hybrid optical-acoustic technologies. *IEEE Access, 9*, 85109-85123. https://doi.org/10.1109/ACCESS.2021.3088467

IEEE Access
Multidisciplinary ⋮ Rapid Review ⋮ Open Access Journal

Received May 17, 2021, accepted June 5, 2021, date of publication June 11, 2021, date of current version June 18, 2021.

Digital Object Identifier 10.1109/ACCESS.2021.3088467

Green Underwater Wireless Communications Using Hybrid Optical-Acoustic Technologies

KAZI YASIN ISLAM[1], (Student Member, IEEE), IFTEKHAR AHMAD[1], (Member, IEEE), DARYOUSH HABIBI[1], (Senior Member, IEEE), M. ISHTIAQUE A. ZAHED[2], AND JOARDER KAMRUZZAMAN[3], (Senior Member, IEEE)

[1]School of Engineering, Edith Cowan University, Perth, WA 6027, Australia
[2]School of Science, Engineering and Technology, East Delta University, Chittagong 4209, Bangladesh
[3]School of Engineering, Information Technology and Physical Sciences, Federation University Australia, Ballarat, VIC 3350, Australia

Corresponding author: Kazi Yasin Islam (kyislam@our.ecu.edu.au)

This work was supported in part by the Department of Jobs, Tourism, Science and Innovation - Defence Science Centre, Australia, under Grant G1005365.

ABSTRACT Underwater wireless communication is a rapidly growing field, especially with the recent emergence of technologies such as autonomous underwater vehicles (AUVs) and remotely operated vehicles (ROVs). To support the high-bandwidth applications using these technologies, underwater optics has attracted significant attention, alongside its complementary technology – underwater acoustics. In this paper, we propose a hybrid opto-acoustic underwater wireless communication model that reduces network power consumption and supports high-data rate underwater applications by selecting appropriate communication links in response to varying traffic loads and dynamic weather conditions. Underwater optics offers high data rates and consumes less power. However, due to the severe absorption of light in the medium, the communication range is short in underwater optics. Conversely, acoustics suffers from low data rate and high power consumption, but provides longer communication ranges. Since most underwater equipment relies on battery power, energy-efficient communication is critical for reliable underwater communications. In this work, we derive analytical models for both underwater acoustics and optics, and calculate the required transmit power for reliable communications in various underwater communication environments. We then formulate an optimization problem that minimizes the network power consumption for carrying data from underwater nodes to surface sinks under varying traffic loads and weather conditions. The proposed optimization model can be solved offline periodically, hence the additional computational complexity to find the optimum solution for larger networks is not a limiting factor for practical applications. Our results indicate that the proposed technique yields up to 35% power savings compared to existing opto-acoustic solutions.

INDEX TERMS Green communication, hybrid networks, optimization, underwater wireless communication.

I. INTRODUCTION

Although modern humans have tamed terrestrial wireless communication to harness numerous benefits, they lack that same prowess in the underwater domain. Interestingly, water covers almost 70% of planet Earth's surface [1] and yet this area is almost unexplored. Over the last few decades, humans have attempted to establish reliable underwater wireless communication (UWC) infrastructures, in order to explore these uncharted territories. However, attaining reliable UWC poses various significant and unique challenges, owing to the highly dynamic nature and inherent properties of the aquatic medium [2]. The first major challenge involves terrestrial radio frequency (RF) technologies being infeasible in the underwater medium due to the severe attenuation of radio waves in water, with worsened effects in conductive ocean water [3].

The second major challenge for wireless communication in the underwater domain relates to its severe energy-constrained nature. Underwater nodes have limited battery energy storage but they need to remain operational during the entire period of their mission lifetime, which could span from several days to a few months or even years. Recharging or replacing the batteries in these nodes is an expensive

The associate editor coordinating the review of this manuscript and approving it for publication was Huaqing Li.

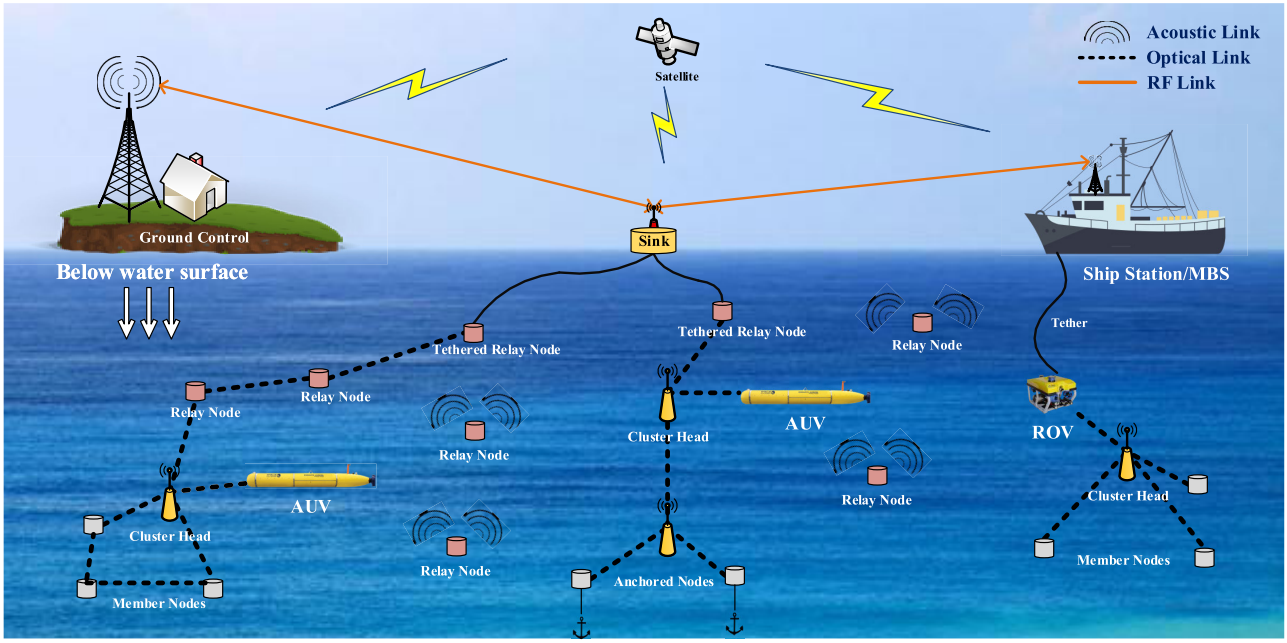

FIGURE 1. Underwater wireless communication scenario.

and challenging task [4]. Therefore, it is vital for these nodes to communicate in an energy-efficient manner.

To tackle these challenges, over the years, researchers have developed other physical (PHY) layer technologies such as underwater acoustic communication (UAC) [5], [6], underwater optical communication (UOC) [1], [2], [7], and underwater magnetic induction communication (UMIC) [8], [9] as alternative UWC techniques. However, each of these techniques possesses its own merits and drawbacks. For instance, UAC offers long-range communication but suffers from low speed, low bandwidth, high energy consumption, and multipath issues. However, unlike UAC, UOC and UMIC offer high speed, high bandwidth, low power communication at the cost of shorter range and lower reliability [10].

With the advent of these new technologies, the UWC field has enjoyed rapid growth in research, business, and defence interests, giving rise to the Internet of Underwater Things (IoUT) [11]. However, a single communication technology is insufficient in meeting the demands posed by the IoUT, as it entails a wide range of applications with varied network performance requirements. These applications include, but are not limited to: offshore oil and gas operations and explorations, military tactical operations, oceanography, and seismology [12].

Recently, many of these applications have required the use of autonomous underwater vehicles (AUVs) and remotely operated underwater vehicles (ROVs) as illustrated in Figure 1. These vessels are deployed underwater to collect data for a certain period of time. The data types may range from low bit rate sensor measurements to high bit rate, high resolution images, or even real-time videos to be transferred at 10,000 MB/hour (≈3 MB/s) [13]. With growing interest in the IoUT, these data rates are projected to increase manyfold in the near future [14].

However, low speed UAC is unable to support these high data rate demands due to the low speed of sound (≈1500 m/s) propagation underwater [15]. Therefore, in order to meet these traffic demands, the natural alternative is to use high speed communication links, such as those provided by UOC using laser diodes (LD), ligh-emitting diodes (LED) or μ-LEDs [16]. As mentioned previously, however, UOC involves certain costs such as short range communication and the requirement for near-perfect transmitter/receiver alignment within turbulent and dynamic underwater conditions. In adverse weather conditions such as turbulent oceans with highly turbid water, UOC suffers from high bit error rates (BER), because optical beams cannot penetrate opaque, murky water [17]. In these scenarios, UAC is a more reliable choice for communication.

To summarize, on a particular day, an underwater wireless communication network (UWCN) can experience varying traffic load based on its diverse applications, where it also encounters dynamic water conditions driven by changing weather. Given these circumstances, one key research question becomes, "what is the most suitable, energy-optimized end-to-end connectivity of an UWCN given the varying traffic demands and dynamic water/weather conditions?" To answer this research question, we propose a hybrid opto-acoustic UWC solution comprised of both UAC and UOC technologies, that selects the most optimal strategy for underwater data transmission for a given traffic load and dynamic water conditions during a certain period of time.

In this work, the water/weather condition is jointly determined by water temperature, pH and salinity affecting transmit power and consequently the required signal-to-noise ratio (SNR) for reliable data transmission by UAC. Contrastingly, water turbidity affects the required SNR threshold for reliable data transmission by UOC. For both UAC and UOC, good water/weather indicates the required SNR to be above a certain SNR threshold for reliable communication, where adverse weather indicates otherwise. In our proposed solution, the network connectivity is optical under heavy traffic load and favorable underwater weather conditions (e.g., less turbid water) in order to support the high traffic demand. For the same weather conditions but with lower traffic, the links can either be acoustic or optical, whichever consumes less power. Conversely, during adverse weather conditions (e.g., highly turbid water affecting UOC and/or other factors affecting UAC), the connectivity is acoustic if the traffic volume is low. However, under high traffic load during adverse weather conditions, both acoustic and optical links need to be jointly activated in order to meet the traffic demand because the transmission channel becomes less reliable in these conditions. Although this may result in a higher power consumption, the network reliability needs to be maintained. We formulate our optimization model to select the most appropriate links (acoustic or optical or both) in response to the changing weather conditions and traffic demands and hence minimizes network power consumption while also satisfying traffic demands.

To the best of our knowledge, our research is the first major work that studies power consumption implications for a hybrid opto-acoustic UWCN that also incorporates the effects of traffic load and weather-dependent phenomena on network connectivity. The major contributions of this paper are as follows:

- We propose a hybrid opto-acoustic UWCN solution aimed at optimizing power consumption, while considering both environmental variations and traffic demands. Our proposed solution is modelled as a binary integer programming (BIP) problem.
- We solve the optimization problem and then compare the performance of our proposed hybrid solution against standalone all-acoustic and all-optical UWCN, and also against a relevant work in the literature, in terms of power consumption and throughput using simulation. The results show our proposed solution delivers significant power savings of up to 35% compared to existing solutions.

The remainder of this paper is organized as follows: we provide a detailed description of the problem in Section II; then we present relevant works in Section III; Section IV presents the system model including the network model, traffic model, and analytical models for channel propagation and noise factors for both UAC and UOC; Section V details the derivation of power consumption expressions for UAC and UOC, and then presents the optimization problem formulation with our proposed power-saving algorithm; This is followed by a presentation of the results and their analysis in Section VI; and finally Section VII summarizes the work presented in this research.

II. PROBLEM DESCRIPTION

An underwater wireless communication network (UWCN) is shown in Figure 1. The underwater network is comprised of several node clusters composed of a few member nodes (MN) and at least one cluster head (CH). Some MNs are floating with weights attached to them, whilst others are anchored to the ocean bed. These MNs collect data based on their assigned applications and forward this data to the CHs. The CHs aggregate traffic from the MNs and attempt to forward the aggregate traffic to the surface sinks (SS) and the ship station/mobile base station (MBS) via relay nodes (RNs), and to the nearby AUVs and ROVs. The RNs sit between the CHs and SS/MBS and assist with increasing the range of communication for short-range optical links, and use multi-hop transmission [18] to forward data. Lastly, the SS/MBS forward the data to ground control (GC) using over-the-air (OTA) radio-frequency (RF) links.

In this scenario, we assume that the CHs are equipped with both acoustic and optical modems for forwarding data to the SS/MBS, using either acoustic or optical links, or both to transmit data based on traffic demand and water/weather conditions. Accordingly, the CHs determine the most optimal link to forward data reliably and energy-efficiently. CHs make this decision by considering the traffic volume and water/weather conditions on a given hour of the day.

As mentioned above, in good weather conditions and with high traffic load, the CHs use high-speed optical links to transmit data towards the GCs. Accordingly, the traffic flows through all-optical links, and no acoustic links are required in this scenario. For the same weather conditions, but with low traffic load, only acoustic links are sufficient to meet the traffic demand, allowing optical RNs to switch into sleep mode. This strategy minimizes the number of active network components and therefore improves the energy efficiency of the network.

In adverse weather conditions, especially with highly turbid water, the CHs use acoustic links to transmit data because the optical links are no longer reliable. In this case also, the optical RNs switch into sleep mode. However, with bad weather conditions and high traffic volume, optical links are required in conjunction with acoustic links in order to satisfy traffic demand, although the links may not be as reliable. Whilst this increases network power consumption, our proposed hybrid solution ensures that the data is transmitted in the most energy-efficient manner. This overall strategy ensures that network power consumption is minimized while traffic demand is also met reliably given variability of weather and traffic conditions on a certain day.

III. RELATED WORKS

Owing to the complementarity of acoustic and optical UWC techniques, a number of research works related to hybrid

opto-acoustic techniques have been published in the literature regarding underwater communications. Vasilescu *et al*. [19] have published one of the earliest works on hybrid UWCNs where UAC is used for low-speed underwater broadcast signals and UOC is used for high-speed point-to-point communication in an underwater sensor network (UWSN). In this work, the authors have demonstrated that it is possible to transmit low resolution images underwater using self-developed hardware. Farr *et al*. [20] have shown in their work that full-duplex UOC links can be used for real-time control of untethered ROVs (UTROVs), such as *Nereus* and *Alvin*. Moreover, they present a conceptual illustration of hybrid optical-acoustic communication links used for data muling and controlling these UTROVs. Later, Hu *et al*. [21] proposed and developed a novel multi-level, Q-learning based routing protocol (MURAO) to facilitate a hybrid acoustic-optical UWCN system. Their algorithm utilized long-range acoustic signals for ranging, route selection and cluster formation purposes, and short-range optical signals for intra-cluster node communication and data transfer operations.

Han *et al*. [22] have demonstrated in their simulation work that a hybrid acoustic-optical communication mode can outperform standalone acoustic modes in terms of energy consumption and throughput. This is one of the first studies to examine power consumption implications for a hybrid UWC system. They used constant bit rate (CBR) traffic for simulation, with packet sizes 1.75 kB and 50 kB for acoustic and optical links, respectively. However, their simulation did not account for any environmental parameters such as water temperature or turbidity that affect communication links.

More recently, Wang *et al*. [23] have incorporated these changing environmental parameters in their work, where they have proposed a hybrid acoustic-optical communication system with two transmission modes: classical acoustic mode and a self-adaptive, multi-hop opto-acoustic mode. Their technique applied the opto-acoustic mode when the SNR was above an acceptable threshold and switched to the classical acoustic mode when the SNR was below that threshold. The performance reported in this work only provides an indication of the transmission distances and data rates achievable by either of these techniques, thereby lacking an in-depth analysis of the achieved performance, especially energy consumption aspects of these technologies. More recently, Mostafa *et al*. [24] have published a comparative study of the four major PHY-layer UWC techniques in terms of energy efficiency and total system throughput. This is one of the first works to attempt to optimize energy efficiency in a hybrid UWCN subject to SNR and number of hop constraints. However, this work did not account for the effects of environmental parameters and only considered fixed-length packet size for traffic, with no variability. A summary of these existing related works has been presented in Table 1.

In summary, none of these previous works have considered both varying traffic volume and dynamic water/weather conditions in their hybrid opto-acoustic approach. Moreover, except for Mostafa *et al*. [24], no other work has attempted to utilize optimization methods to minimize power consumption in UWCNs. To the best of our knowledge, our research is the first major work that undertakes an optimization of power consumption in hybrid opto-acoustic UWCNs, whilst incorporating the effects of variable traffic load and dynamic water/weather conditions.

TABLE 1. Summary of existing works on underwater hybrid optical-acoustic technologies.

Research Work	Hybrid Optical-Acoustic Technology	Energy Consideration	Traffic Variability	Dynamic Environmental Parameters
[19]	✓	x	x	x
[20]	✓	x	x	x
[21]	✓	x	x	x
[22]	✓	✓	✓	x
[23]	✓	x	x	✓
[24]	✓	✓	x	x
Proposed	✓	✓	✓	✓

IV. PROPOSED SYSTEM MODEL

We present our proposed system model in this section. At first, we develop the overall network model comprised of the underwater hybrid opto-acoustic network and an underwater traffic model for this network. Next, we develop analytical models to calculate channel propagation loss and channel noise for both UAC and UOC networks.

A. NETWORK MODEL

Figure 2 depicts a hybrid opto-acoustic UWCN system. This model is composed of a set of nodes $\mathcal{V}$, including a surface sink/base station ($n = 0$) and $N - 1$ nodes ($n = 1, 2, \ldots, N$) including cluster heads. The cardinality of this set $\mathcal{V}$ is represented by N. The nodes are arranged in $M_{cluster}$ that are represented by the set $m = 1, 2, \ldots, M_{cluster}$. For each cluster m, we consider a different network topology including ring, star, and tree configurations.

Within each cluster, the MNs can communicate with each other and with the CHs using high-speed, low-power, short-range optical links. Sensor nodes, AUVs, and ROVs can all be treated as MNs. Once data from MNs are aggregated at CHs, hybrid opto-acoustic links are available to CHs for further data transfer, either to RNs or to the BS/SS depending on traffic demand and water/weather conditions. The BS/SS are in turn connected to on-shore ground control and satellites with OTA RF links.

B. TRAFFIC MODEL

Our traffic model consists of three traffic types: constant bit rate (CBR), variable bit rate (VBR), and best effort (BE) traffic. These traffic types are generated by a variety of IoUT applications as discussed in the later part of this subsection. We consider an hourly traffic flow over a period of six days. Similar to the works in [25]–[28], Figure 2b illustrates the normalized hourly traffic load profile for one day.

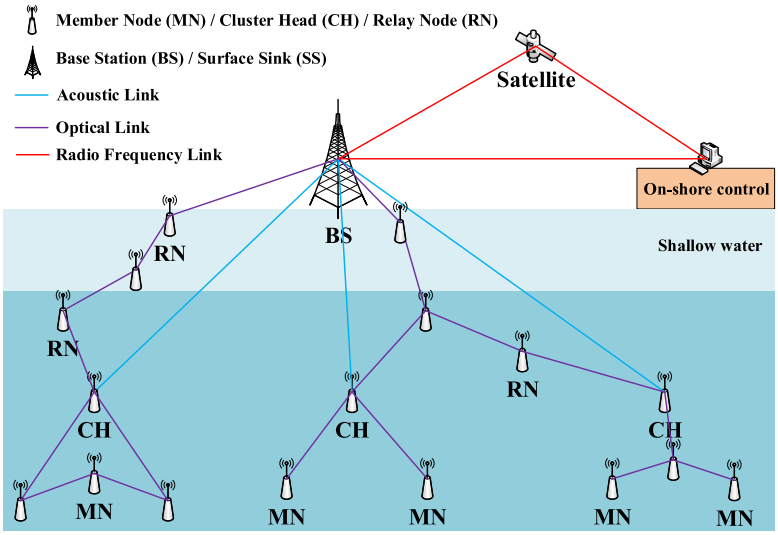

(a) System model (AUVs and ROVs can be treated as MNs).

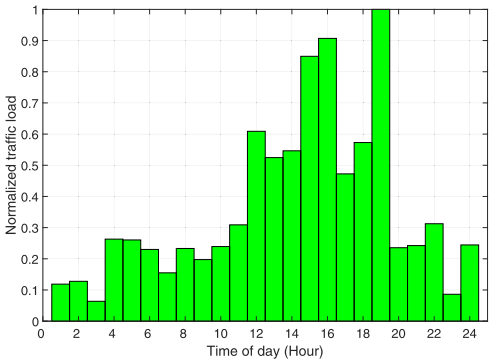

(b) Normalized underwater traffic load over a 24-hour period.

FIGURE 2. **The network model.**

To model and synthesize the varying underwater network traffic load shown in Figure 2b, we consider various IoUT applications discussed in [12], [29]–[31] that can generate a varying traffic demand. For instance, scientific measurements involving periodic recordings of temperature, pH, and salinity by underwater sensors and the transfer of these data are low data rate applications. On the other hand, real-time, high resolution image and/or video transfer by AUVs and ROVs are high data rate applications. Considering these various types of projects that may be conducted throughout a day (for 24 hours) in the underwater domain, we constructed an approximate variation of the traffic load that an underwater network is required to service, and hence support these various IoUT applications.

To model this network traffic, we consider both periodic and non-periodic data collection required for the purposes of a variety of IoUT applications including oil and gas, military, oceanography, and seismology. Additionally, we consider the scenario where AUVs and ROVs are deployed underwater for ocean column and bottom monitoring during specific times on certain days over a 6-day period [32].

When these marine vehicles are deployed, they often transfer high resolution images and real-time videos over the network, resulting in a high traffic load. An example of this scenario is reflected during the hours 12:00 to 19:00 in Figure 2b. AUVs are operational during these five hours and are transmitting high-data rate content such as images and videos, resulting in an increased traffic demand during these five hours compared to other hours of the day. The demand peaks at 19:00 because before wrapping up the operation for the day and returning to the base, the activities in AUVs typically increase in the final hour, resulting in higher volume of traffic.

C. WEATHER DATA

In order to investigate the effects of changing weather conditions underwater on UWCNs, we extracted temperature, salinity, and pH data from the dataset "Mumford Cove Monitoring Data" [33] (dataset 1). The researchers investigating these water properties in dataset 1 recorded them at 30-minute intervals in Mumford Cove, CT (41 degrees 19′25″N, 72 degrees 01′07″W). This dataset includes measurements from 14 April 2015 to 04 February 2020. Accordingly, we have extracted records for six days from 01 September 2019 to 06 September 2019 for use in our work.

Since one of our main objectives in this work is to evaluate the performance of our proposed optimization model under varying environmental conditions, we found that six instances (i.e., six days of data) from dataset 1 provide us with sufficient amount of fluctuations in the environmental parameters to validate the proof of concept, as shown in Figures 3a, 3b, and 3c. The six-day variation in water temperature, salinity, and pH respectively allows us to perform our investigations and meet the objective for this work. These three parameters largely affect UAC.

For UOC, we considered a different dataset "Reciprocal transplant expt. - irradiance and light attenuation 2017" [34] (dataset 2), which provided us optical extinction coefficient data in Varadero Reef, Colombia. We used dataset 2 for UOC because dataset 1 contains parameters (temperature, pH, and salinity) that affect UAC only. To conduct the investigation in this paper, we require environmental parameters that affect UOC as well. Since dataset 1 does not contain any parameter that affects UOC, we used dataset 2 which contains recordings of optical absorption coefficient that impacts UOC. Therefore, we used both datasets in our investigation — dataset 1 for its effects on the acoustic component, and

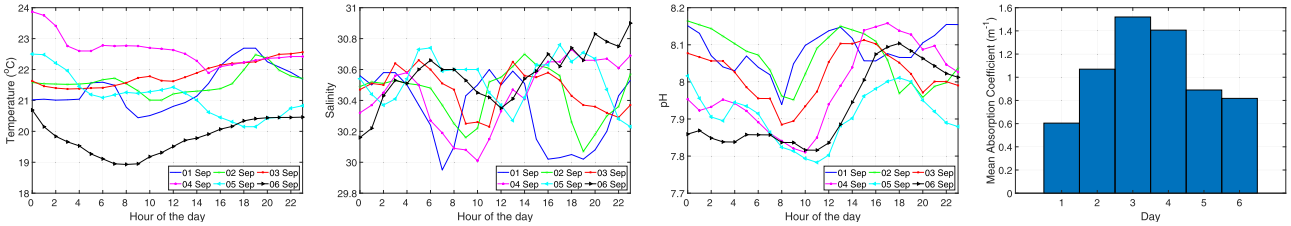

(a) Temperature (°C) (b) Salinity (c) pH (d) Mean optical absorption coefficient (m^{-1})

FIGURE 3. Environmental variables used in the proposed hybrid opto-acoustic solution.

dataset 2 for its effects on the optical component of the hybrid solution.

Although the recordings of dataset 2 are not taken at the same geographical location as dataset 1, without the loss of generality, measurements found in dataset 2 provide a reasonable understanding of how the optical attenuation parameter may vary over a certain period. Figure 3d presents the mean optical extinction coefficient data over a period of 6 days.

D. ACOUSTIC CHANNEL PROPAGATION MODEL

In this section, we describe the analytical model we developed for UAC channel propagation based on the works [22], [35]–[37].

The total path loss for UAC due to absorption and spreading is given by [38]

$$A_{ac}(d,f) = A_0 \cdot d^k \cdot \alpha(f)^{d_{km}} \tag{1}$$

where the term A_0 accounts for a normalisation factor (NF) which relates to the inverse of the transmitted power; d^k accounts for the spreading loss over the distance d (m) between the transmitter and receiver, and k denotes the path loss exponent (1 for cylindrical, 2 for spherical, and 1.5 for practical spreading); and the term $\alpha(f)^{d_{km}}$ denotes the absorption coefficient (dB/km) that accounts for the absorption loss over a distance $d_{km} = d \times 10^{-3}$ given in km.

The total UAC path loss in dB can be expressed as

$$10\log A_{ac}(d,f) = 10\log A_0 + k \cdot 10\log d + d_{km} \cdot 10\log \alpha(f) \tag{2}$$

It is to be noted that the absorption coefficient $10\log\alpha(f)$ is not only a function of the acoustic signal frequency f, but also a function of water salinity S, water temperature T, water pH, water depth z, and the speed of acoustic wave propagation c. The speed of acoustic wave propagation c can be calculated by [39]

$$c = 1412 + 3.21T + 1.19S + 0.0167z \tag{3}$$

Several expressions for calculating the absorption coefficient $10\log\alpha(f)$ are available in the literature. The most widely used model is Thorp's empirical formula [39]. However, Thorp's expression is only applicable for lower water temperatures, and also it does not capture the effects of water salinity, temperature, pressure, speed of sound, and depth. A more accurate model has been proposed by Francois and Garrison [40], [41] that encapsulates oceanographic factors within the frequency range 100 Hz $< f <$ 1 MHz is given by

$$\alpha(f) = \frac{A_1 P_1 f_1 f^2}{f^2 + f_1^2} + \frac{A_2 P_2 f_2 f^2}{f^2 + f_2^2} + A_3 P_3 f^2 \tag{4}$$

where the first term describes the ionic relaxation effects caused by the presence of boric acid (H_3BO_3) molecules, the second term describes the effects due to the magnesium sulfate ($MgSO_4$) salt concentration, and the third term describes the viscous absorption component due to pure water. A detailed breakdown of the terms used in equation (4) and their relationship with the aforementioned water properties is provided in Appendix A.

For realistic underwater acoustic propagation modeling, we have used (4) to model the acoustic absorption loss in this paper.

E. ACOUSTIC NOISE MODEL

In addition to attenuation factors, UAC also suffers from various sources of underwater noise. Ambient underwater noise affecting water acoustics can be categorized according to the frequency range in which their effects are most prominent. Based on the works [38] and [42], a generic ambient (but not site-specific) noise model can be approximated from the common sources of noise using Gaussian statistics and a continuous power spectral density (PSD). These noise sources are described as follows [43]:

1) Turbulence noise, $N_t(f)$ - Occurs due to the oceanic wave turbulence. This noise is the most prominent in the $f <$ 10 Hz band and is given by

$$10\log N_t(f) = 17 - 30\log f \tag{5}$$

2) Shipping/Vessel noise, $N_s(f)$ - Dominant within the band 10 $< f <$ 100 Hz, this ambient noise is generated by shipping and vessel activities on the water, and is expressed as

$$10\log N_s(f) = 40 + 20(s - 0.5) + 26\log f - 60\log(f + 0.03) \tag{6}$$

where $s \in [0, 1]$ is the shipping activity factor, with 0 indicating low shipping activity and vice versa.

3) Wave noise, $N_w(f)$ - Generated by the water surface wave motion caused by wind and is most prominent in the 100 Hz $< f <$ 100 kHz range. This noise component is given by

$$10\log N_w(f) = 50 + 7.5\sqrt{w} + 20\log f - 40\log(f + 0.4) \quad (7)$$

where w is the wind speed in m/s.

4) Thermal noise, $N_{th}(f)$ - Occurs above the frequency range of $f > 100$ kHz due to thermal agitation caused by pressure fluctuations in the ocean. This provides the lowest bound for ambient noise levels in the ocean and is given by

$$10\log N_{th}(f) = -15 + 20\log f \quad (8)$$

The overall noise PSD $N_{Total}(f)$ in dB re 1μPa per Hz is given by [24], [42], [44]

$$N_{Total}(f) = N_t(f) + N_s(f) + N_w(f) + N_{th}(f) \quad (9)$$

F. OPTICAL CHANNEL PROPAGATION MODEL

Light attenuation occurs underwater due to the following phenomena:

1) Absorption - Occurs when light energy is converted to heat energy via collision with water molecules, salt molecules, chlorophyll, and other organic matter found underwater. The absorption coefficient is denoted by $a(\lambda)$, where λ is the wavelength of the optical beam.
2) Scattering - Occurs due to salt ions and particulate matter dissolved in the water. The scattering coefficient is denoted by $b(\lambda)$.

Considering both absorption and scattering, the underwater optical beam extinction coefficient $c(\lambda)$ can be formulated as [36], [45]

$$c(\lambda) = a(\lambda) + b(\lambda) \quad (10)$$

We used beam extinction coefficient ($c(\lambda)$) data from the Varadero dataset (dataset 2) to calculate the propagation loss factor $l(d, \lambda)$ using

$$l(d, \lambda) = \exp(-c(\lambda)d) \quad (11)$$

Next, we calculated total optical path loss $L_{op}(d, \lambda)$ due to absorption and scattering for line-of-sight (LOS) optical links based on the work in [46]

$$L_{op}(d, \lambda) = \frac{A_r n_t n_r cos\theta}{2\pi d^2(1 - cos\theta_0)} \cdot \exp(-c(\lambda)d) \quad (12)$$

where A_r is the receiver aperture, n_t and n_r are the optical efficiencies of the transmitter and receiver respectively, θ is the inclination angle between the transmitter and receiver, and θ_0 is the beam divergence angle of the transmitter.

From [46], the total optical channel attenuation or channel gain $H_{op}(d, \lambda)$ can be expressed as

$$H_{op}(d, \lambda) = \alpha_{op}^2 \cdot L(d, \lambda) \quad (13)$$

where α_{op}^2 is the optical fading amplitude due to water turbulence and can be modelled as a log-normal distribution with a probability distribution function (PDF) of

$$f(\alpha) = \frac{1}{\alpha\sqrt{2\pi\sigma_X^2}} \cdot \exp\left(-\frac{(\ln(\alpha) - \mu_X)^2}{2\sigma_X^2}\right) \quad (14)$$

where the random variable X is the fading log-amplitude that follows Gaussian distribution with mean μ_X and variance σ_X^2.

G. OPTICAL NOISE MODEL

In addition to path loss due to absorption and scattering, underwater optical signals also suffer from various types of noise. These noise types can be categorised as follows [36], [46]–[48]:

1) Thermal/Johnson noise - Noise variance can be expressed as

$$\sigma_{TH}^2 = \frac{4k_B \cdot T_e \cdot F \cdot B}{R_L} \quad (15)$$

where k_B is the Boltzmann constant (1.38×10^{-23} J/K), T_e is the equivalent temperature (290 K), F is the system noise figure ($F = 4$), B is the electronic bandwidth, and R_L is the load resistance.

2) Dark current noise - Caused by electrical current leakage from the photo-detector at the receiver side of the communication system. This can be expressed as

$$\sigma_{DC}^2 = 2q \cdot I_{DC} \cdot B \quad (16)$$

where q is the charge of an electron (1.602×10^{-19} C) and I_{DC} is the reverse leakage current of a photo-diode (1.23×10^{-9} A).

3) Quantum/Signal shot noise - Arises out of the random photon number variations at the receiver and is formulated as

$$\sigma_{SS}^2 = 2q \cdot \rho \cdot P_i \cdot B \quad (17)$$

where ρ is the responsivity of the photo-diode and P_i is the signal power.

4) Background noise - Consists of noise due to ambient, refracted sunlight from the water surface and the blackbody radiation. This can be expressed as

$$\sigma_{BG}^2 = 2q \cdot \rho \cdot P_{BG} \cdot B \quad (18)$$

where P_{BG} is the background noise power and can be expressed as

$$P_{BG} = P_{solar} + P_{blackbody} \quad (19)$$

P_{solar} can be written as

$$P_{solar} = A_r \cdot \pi(FOV)^2 \cdot \Delta\lambda \cdot T_F \cdot L_{sol} \quad (20)$$

where A_r is the receiver aperture, FOV is the receiver field of view, $\Delta\lambda$ is the optical filter bandwidth, T_F is

the optical transmissivity, and L_{sol} is the solar radiance. Similarly, $P_{blackbody}$ can be written as

$$P_{blackbody} = \frac{2hc^2\alpha \cdot \pi(FOV)^2 \cdot A_r T_A T_F \Delta\lambda}{\lambda^5 \cdot \left[\exp\left(\frac{hc}{\lambda kT}\right) - 1\right]} \quad (21)$$

where h is Planck's constant (6.62×10^{-34} m^2 kg/s), c is the speed of light underwater (2.25×10^8 m/s), α is the radiant absorption factor (0.5), T_A is the transmission in water ($T_A = \exp(-\tau_0)$, where τ_0 is the atmospheric transmission), and λ is the wavelength of the optical beam.

Each of these noise sources are independent of one another and can be represented as additive white Gaussian noise (AWGN). This means that total optical noise can also be modelled as AWGN with zero mean and variance σ^2 [46]. The total optical noise can then be expressed as

$$\sigma^2_{total} = \sigma^2_{TH} + \sigma^2_{DC} + \sigma^2_{SS} + \sigma^2_{BG} \quad (22)$$

V. POWER CONSUMPTION AND PROBLEM FORMULATION

In the first two parts of this section, we present the power consumption models for both UAC and UOC networks we used in our proposed solution. We formulate our optimization problem in terms of a UWCN in the last part of this section.

A. ACOUSTIC POWER CONSUMPTION MODEL

To formulate the power consumption model of the proposed underwater network, we define the set $T = (t_1, t_2, \ldots, t_i)$ consisting of i transmitter nodes. Next, we define another set $R = (r_1, r_2, \ldots, r_j)$ of j receiver nodes. We denote the ith transmitter node as t_i, and the jth receiver node as r_j. We then formulate the received acoustic signal power $P^r_{j,ac}$ at the jth receiver node as

$$P^r_{j,ac} = P^t_{i,ac} \cdot A^{-1}_{ij,ac} \quad (23)$$

where $P^t_{i,ac}$ is the transmit acoustic power at the transmitter node t_i, and $A_{ij,ac}$ is the acoustic channel attenuation or channel gain from (1) for the path $i \rightarrow j$.

Next, we formulate the signal-to-noise ratio (SNR) $\gamma^r_{j,ac}$ at the receiver node r_j as

$$\gamma^r_{j,ac} = \frac{P^r_{j,ac}}{N_{ij,Total} \cdot B_j} \quad (24)$$

where $N_{ij,Total}$ is the total ambient noise PSD derived in (9) for the path $i \rightarrow j$ and B_j is the receiver noise bandwidth.

Then, substituting (23) to (24) and re-arranging, we derive an expression for the acoustic transmit power at node t_i which is given as

$$P^t_{i,ac} = \gamma^r_{j,ac} \cdot A_{ij,ac} \cdot N_{ij,Total} \cdot B_j \quad (25)$$

Based on the hourly underwater communication traffic load, we estimate a target acoustic SNR that must be achieved by the acoustic links to ensure reliable data transmission. This target acoustic SNR is calculated using

$$\gamma^{r,target}_{j,ac} = 10\log\left(2^{\frac{C^{daily}}{B_{ac}}} - 1\right) \quad (26)$$

where, C^{daily} is the daily traffic load (Mbps) and B_{ac} is the acoustic link bandwidth (kHz).

Thus, the transmit power required to meet a threshold SNR in UACs with a centre frequency f within a distance d can be formulated as [49]

$$P^t_{i,ac}(d,f) = \gamma^{r,target}_{j,ac} \cdot A_{ij,ac}(d,f) \cdot N_{ij,Total}(d,f) \cdot B_j(f) \quad (27)$$

B. OPTICAL POWER CONSUMPTION

Making similar assumptions as subsection (V-A), the optical signal power $P^r_{j,op}$ at the receiver node r_j can be given by

$$P^r_{j,op} = P^t_{i,op} \cdot H_{ij} \quad (28)$$

where $P^t_{i,op}$ is the optical power at the transmitter node t_i, and H_{ij} is the optical channel attenuation or channel gain for the path $i \rightarrow j$ from (13).

Next, let the optical SNR $\gamma^r_{j,op}$ at the receiver node r^r_j be

$$\gamma^r_{j,op} = \frac{(P^r_{j,op})^2 \cdot \rho^2}{\sigma^2_{j,total}} \quad (29)$$

where ρ is the responsivity of the photo-detector at the receiver and $\sigma^2_{j,total}$ is the total noise variance for the path $i \rightarrow j$ derived in (22). Then, substituting (28) into (29), we obtain

$$\gamma^r_{j,op} = \frac{(P^t_{i,op})^2 \cdot H^2_{ij} \cdot \rho^2}{\sigma^2_{j,total}} \quad (30)$$

Similar to acoustic SNR, we calculate the target optical SNR [48], [50] using

$$\gamma^{r,target}_{j,op} = 10\log\left(2^{\frac{C^{daily}}{B_{op}}} - 1\right) \quad (31)$$

where, C^{daily} is the daily traffic load (Mbps) and B_{op} is the optical link bandwidth (MHz).

Thus, re-arranging (30) and using (31) we derive an expression for the optical transmit power at node t_i which is given by

$$P^t_{i,op} = \sqrt{\frac{\gamma^{r,target}_{j,op} \cdot \sigma^2_{j,total}}{H^2_{ij} \cdot \rho^2}} \quad (32)$$

C. OPTIMIZATION PROBLEM FORMULATION

To minimize the overall power consumption of the proposed hybrid UWCN, we define an optimization problem. We formulate the problem as a binary integer programming (BIP) where the objective is to minimize the total power consumption (cost) of the UWCN. The input to this optimization model is the hourly network traffic demand and weather conditions. These variations, when expressed in hours, are more noticeable and hence, the impacts on power consumption can be better quantified. Based on these variations in the input,

the optimization model calculates the most optimal (most energy-efficient) strategy for data transmission from the data collection nodes at the bottom part of the ocean to the surface base stations, and thus is expected to minimize network power consumption. When considering the network point-of-view, this problem can be identified as analogous to a minimum network cost flow (MNCF) problem [51].

The problem can be translated into a network with a directed, weighted graph $\mathcal{G} = (\mathcal{V}, \mathcal{E})$, where $\mathcal{V}$ represents all network vertices/nodes (MN, CH, RN, and BS) and $\mathcal{E}$ represents all edges/links (acoustic or optical) between these vertices. To formulate the problem, let the source vertex be i and the destination vertex be j. Moreover, let $u_{ij} \geq 0$ denote the capacity of the link $(i, j) \in \mathcal{E}$, and let $\mathcal{R}$ be the set of traffic demands. Demand $r \in \mathcal{R}$ must send a traffic volume of ϕ^r from a source $s(r)$ to a destination $d(r)$.

In this problem, the network cost is power consumption. We denote the node cost by z_i which is the circuit processing power consumed in node i, and we denote link cost by z_{ij} which is the transmit power for the link $(i, j) \in \mathcal{E}$. To summarize, each network vertex $i \in \mathcal{V}$ carries a node cost z_i and each network edge $(i, j) \in \mathcal{E}$ carries a link cost z_{ij} per unit traffic flow through the link $i \rightarrow j$.

For each $i \in \mathcal{V}$ and $(i, j) \in \mathcal{E}$, we introduce two binary variables y_i and x_{ij} that represent the power status (ON/OFF) of node i and link ij respectively. Decision variable y_i determines if a node is active and x_{ij} determines if a link is active by switching between 0 and 1. Therefore,

$$y_i = \begin{cases} 1, & \text{if node } i \text{ is activated for data transfer,} \\ 0, & \text{otherwise.} \end{cases} \tag{33}$$

$$x_{ij} = \begin{cases} 1, & \text{if link } ij \text{ is activated for data transfer,} \\ 0, & \text{otherwise.} \end{cases} \tag{34}$$

The power consumption Z_i by the node i when it is activated for data transmission can then be calculated as

$$Z_i = z_i \cdot y_i \tag{35}$$

where z_i is the circuit processing power for node i, given in Joules per second and y_i is the binary variable taking values 0 or 1.

Furthermore, for each $r \in \mathcal{R}$ and $(i, j) \in \mathcal{E}$, let the continuous positive variable f_{ij}^r denote the rth flow of traffic flow through the link $i \rightarrow j$. Then, the link power consumption Z_{ij}^r for this graph can be calculated as

$$Z_{ij}^r = z_{ij} \cdot f_{ij}^r \tag{36}$$

where z_{ij} is the transmit and receive power required for transmitting and receiving 1 bit of data respectively, given in Joules per bit; f_{ij}^r is the rth traffic flow through the link $i \rightarrow j$, given in bits per second; and Z_{ij}^r denotes the power consumption of the link $i \rightarrow j$ while it is activated for the transmission and/or reception of data, and is given in Joules per second (watts).

Based on these derivations, the overall network power consumption is then given by the summation of all the node power consumption Z_i and the summation of all the link power consumption Z_{ij}^r. Therefore, the optimization problem with its objective function and constraints can then be formulated as follows:

$$\text{minimize} \quad \sum_{i \in \mathcal{V}} Z_i + \sum_{(i,j) \in \mathcal{E}} \sum_{r \in \mathcal{R}} Z_{ij}^r \tag{37}$$

$$\text{subject to} \quad \sum_{(i,j) \in \mathcal{E}} f_{ij}^r - \sum_{(j,i) \in \mathcal{E}} f_{ji}^r = \begin{cases} \phi^r, & \text{if } i = s(r), \\ -\phi^r, & \text{if } i = d(r), \\ 0, & \text{otherwise} \end{cases} \quad \forall i \in \mathcal{V},\ \forall r \in \mathcal{R} \tag{38}$$

$$x_{ij} \geq y_i + y_j - 1, \quad \forall i \in \mathcal{V}, \forall (i, j) \in \mathcal{E} \tag{39}$$

$$x_{ij} \leq y_i, \quad \forall i \in \mathcal{V}, \forall (i, j) \in \mathcal{E} \tag{40}$$

$$x_{ij} \leq y_j, \quad \forall i \in \mathcal{V}, \forall (i, j) \in \mathcal{E} \tag{41}$$

$$0 \leq f_{ij}^r \leq u_{ij} x_{ij}, \quad \forall r \in \mathcal{R}, \forall (i, j) \in \mathcal{E} \tag{42}$$

$$\gamma_{ij}^{ac} \geq \gamma_{j,ac}^{r,target}, \quad \forall (i, j) \in \mathcal{E} \tag{43}$$

$$\gamma_{ij}^{op} \geq \gamma_{j,op}^{r,target}, \quad \forall (i, j) \in \mathcal{E} \tag{44}$$

where (37) is the objective function of the optimization problem which minimizes the overall network cost (network power consumption). The first summation term in (37) is the total node power consumption, and the second summation term in (37) is the total link power consumption derived from (35) and (36) respectively. Constraint (38) is the classical network flow conservation constraint that ensures the network flow is conserved for a given traffic demand ϕ^r through the link $i \rightarrow j$. The first summation in this constraint represents the total flow out of node i, whereas the second summation represents the total flow into node i, and therefore, the difference between these two terms is the net flow generated at this node. The net flow is positive if i is a source node $s(r)$, and it is negative if i is a destination node $d(r)$. The net flow is 0 if i is a transshipment node. Constraint (38) also satisfies the condition where there is a transmitting end, there must be a receiving end.

Furthermore, constraints (39)–(41) ensure that a link $i \rightarrow j$ is activated only if the nodes i and j are switched ON. In other words, these constraints confirm link activeness when the corresponding source and destination nodes are active. Constraint (42) is the classical capacity constraint that ensures that the traffic flow through an active link does not exceed the capacity of that link. It ensures that the maximum traffic flow through a an active link is lower or equal to the link capacity u_{ij}. Lastly, constraints (43) and (44) ensure that acoustic and optical link SNRs meet their corresponding target SNRs.

This optimization problem is a binary integer programming (BIP) [52] problem and belongs to the class of NP-hard problems. We use IBM ILOG CPLEX Optimization Studio [53] to solve this BIP problem and find its exact, optimal solution using our proposed algorithm (Algorithm (1)).

Algorithm 1 Optimized Power Consumption

Input: Weather Data, Traffic Data
Output: Minimized Total Network Power Consumption
for each day [d ∈ 1, 2, ⋯, 6] **do**
  for each hourly [h ∈ 1, 2, ⋯, 24] traffic load and weather data (T_h^d, pH_h^d, S_h^d, $c(\lambda)_h^d$) **do**
    Calculate c from (3)
    if $T_h^d \leq 20$°C **then**
      Calculate A_3 from (51b)
    else
      Calculate A_3 from (51c)
    end if
    Calculate acoustic parameters $\alpha(f)$, $A_{ac}(d,f)$, $N_{Total}(f)$, $\gamma_{j,ac}^{r,target}$, and $P_{i,ac}^t(d,f)$ from (4), (2), (9), (26), and (27) respectively
    Calculate optical parameters $L_{op}(d,\lambda)$, σ_{total}^2, $\gamma_{j,op}^{r,target}$, and $P_{i,op}^t(d,\lambda)$ from (12), (22), (31), and (32) respectively
    if link capacity = TRUE **then**
      if $P_{i,ac}^t(d,f) > P_{max\_modem,ac}^t(d,f)$ **then**
        if $P_{i,op}^t(d,\lambda) > P_{max\_modem,op}^t(d,\lambda)$ **then**
          Terminate
        else
          Store $P_{i,op}^t(d,\lambda)$
        end if
      else if $P_{i,op}^t(d,\lambda) \leq P_{max\_modem,op}^t(d,\lambda)$ **then**
        Store min $\left\{P_{i,ac}^t(d,f), P_{i,op}^t(d,\lambda)\right\}$
      end if
      Solve the optimization problem from (37) subject to constraints (38), (39), (40), (41), (42), (43), and (44)
    else
      No optimal solution found, return ∞
    end if
  end for
end for

Algorithm (1) presents our proposed algorithm, providing a summary of the procedure of our algorithm to minimize the power consumption of a hybrid opto-acoustic UWCN. This algorithm requires the parameter settings presented in Table 2 to calculate the minimized power consumption of the network. These parameter values are taken from a range of sources in the literature, which are provided in Section IV. We used Matlab R2019b on a PC with Intel Xeon E3-1240 3.5-GHz processor with 16-GB RAM to calculate the parametric values required by our proposed algorithm.

The input to this algorithm are the weather data (temperature, salinity, pH, and optical absorption coefficient) from the collected datasets and the traffic model we presented in Section IV. The output of this algorithm is the most optimal mix of acoustic and optical links for transmitting data traffic from the network MNs to the GC resulting in minimized total network power consumption. This output is obtained by directing underwater network traffic through the most optimal combination of the least power-consuming, most reliable links, whilst also accounting for dynamic weather conditions and changing traffic load.

TABLE 2. Parameter settings used in the proposed algorithm.

Symbol	Quantity	Value
d	Transmission Distance	1-100 m
k	Acoustic Path Loss Exponent	1.5
s	Shipping Activity Factor	0.5
w	Wind Speed	10 m/s
B_j	Acoustic Receiver Narrow Bandwidth	5 kHz
A_r	Optical Receiver Aperture	0.01 m^2
n_t	Optical Transmitter Efficiency	0.9
n_r	Optical Receiver Efficiency	0.9
θ	Inclination Angle between Transmitter & Receiver	10°
θ_0	Divergence Angle of Optical Transmitter Beam	10°
B	Electronic Noise Bandwidth	5 MHz
R_L	Load Resistance	100 Ω
ρ	Responsivity of the Photo-Diode	386 μA/W
FOV	Field-of-View of Optical Receiver	10°
$\Delta\lambda$	Optical Filter Bandwidth	30 nm
T_F	Optical Filter Transmissivity	0.95
E	Downwelling Spectral Irradiance	1440 W/m^2
R	Reflectance of E	0.0125
L_{fac}	Directional Dependence of Underwater Radiance	2.9
λ	Optical Beam Wavelength	532 nm
t_0	Atmospheric Transmission	0.37
T	Earth Object Blackbody Temperature	252 K

We implemented this algorithm for a network topology presented in Figure 2. The network topology contains 18 nodes deployed in a 1000 m × 1000 m underwater area at various depths. Sensor nodes, AUVs, and ROVs are all treated as MNs. Several of these MNs make up one cluster. We consider a different network topology for each cluster including ring, star, and tree configurations. Within each cluster, MNs can communicate with each other and with the CHs using high-speed, low-power, short-range optical links. Once data from MNs is aggregated at CHs, hybrid opto-acoustic links are available to CHs for further data transfer either to RNs or to the BS/SS, depending on the traffic demand and water/weather conditions. Our optimization model determines the most optimal combination of acoustic and optical links to be used for data transfer such that power consumption is optimized.

For each hour in a day, our algorithm calculates acoustic parameters from equations (4), (2), (9), (26), and (27) and optical parameters from equations (12), (22), (31), and (32) respectively. Then the algorithm determines if the link capacity is sufficient for a given traffic demand. Once link capacity is confirmed, the algorithm ensures the required acoustic transmit power $P_{i,ac}^t(d,f)$ to maintain a target SNR does not exceed the maximum transmit power of the acoustic modem. If it does exceed, then our algorithm attempts to determine if the optical transmit power $P_{i,op}^t(d,\lambda)$ to maintain a target SNR does not exceed the maximum transmit power of the

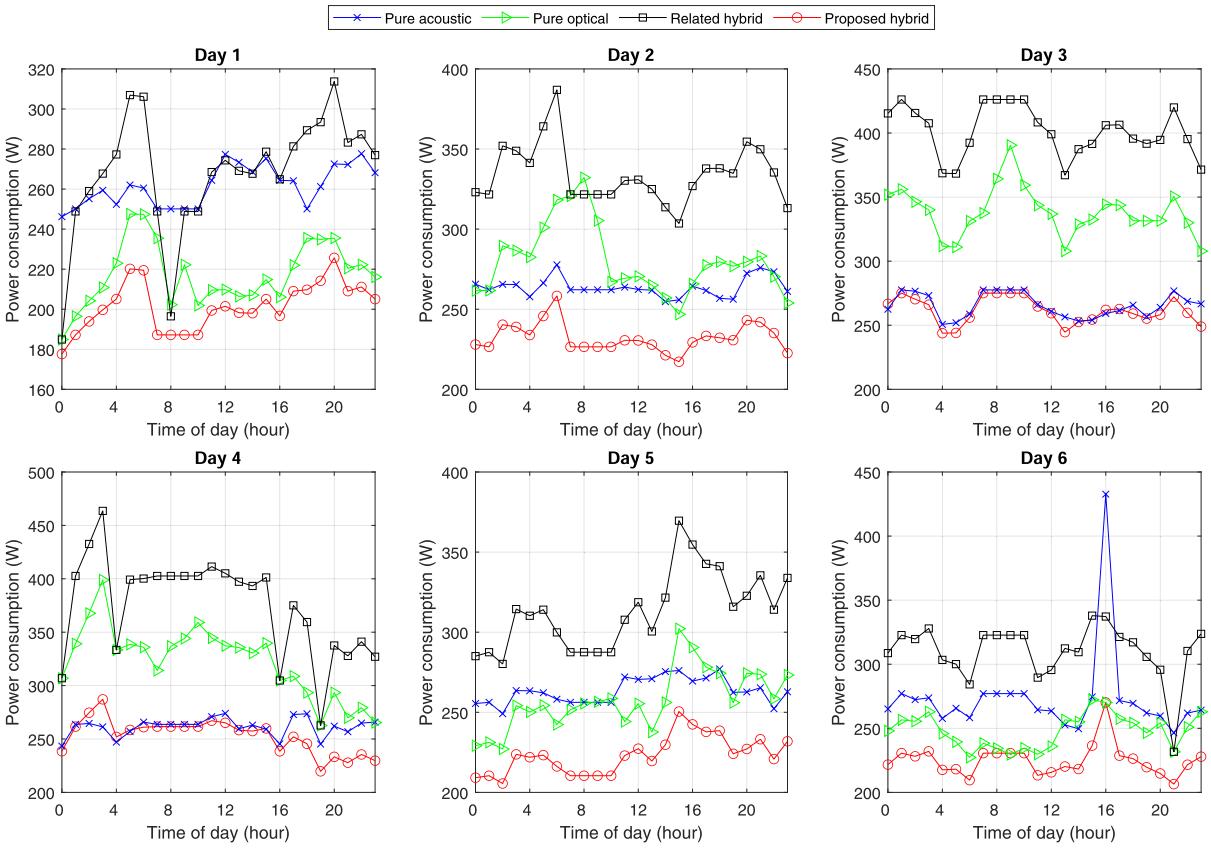

FIGURE 4. Comparison of pure acoustic, pure optical, related hybrid [23], and the proposed hybrid opto-acoustic solution in terms of power consumption (W).

optical modem. If it does exceed, the program terminates. But if the transmit powers do not exceed the maximum modem transmit power, the minimum out of acoustic or optical transmit power is stored, and fed into the optimization model. Next, the optimization model solves the BIP problem with the objective function (37) subject to constraints (38), (39), (40), (41), (42), (43), and (44) to determine the most optimal mix of acoustic and optical links for transmitting data traffic from the network MNs to the GC resulting in the minimized total network power consumption.

As discussed above, our algorithm optimizes the power consumption of an underwater network for each hour during a 6-day period. However, the 6-day period can be extended to any duration depending on the lifetime of the corresponding operation. This technique can be utilized as part of the planning component for an underwater mission carried out by any relevant stakeholder to minimize network power consumption without compromising the reliability of a network due to turbulent weather conditions or high traffic loads.

VI. RESULT ANALYSIS AND DISCUSSION

We present our results in this section with a detailed analysis of the power consumption and average throughput performance metrics of our proposed solution. Figure 4 presents the overall power consumption in the UWCN for four cases: pure acoustic, pure optical, a related hybrid opto-acoustic scheme from [23], and our proposed hybrid opto-acoustic approach.

Pure acoustic indicates that the UWCN uses only acoustic links to transmit data, while pure optical involves using only optical links to transmit data. When the network is purely optical, more RNs are required to relay the data and increase the communication range. This results in an increase in the number of active network components. Although individual UOC modems consume less power compared to UAC modems in transmitting the same amount of data, an increase in the number of RNs for purely optical networks results in higher overall network power consumption.

We choose [23] to be compared with our work because it is the closest and fairest comparative work. As we highlighted in Section III, to the best of our knowledge, our work is the first major work that tackles a power optimization problem in a hybrid opto-acoustic UWCN that considers both environmental parameters and changing traffic conditions. However, authors in [23] implemented a hybrid opto-acoustic scheme which took into account the environmental parameters to determine whether the channel SNR is suitable for transmitting data with high-speed optical links or low-speed acoustic links, which is similar to our proposed technique. Hence, we have used their work for this comparative analysis.

The comparison for power consumed by pure acoustic, pure optical, related hybrid work in [23], and our proposed hybrid solution over the period of 6 days is presented in Figure 4. From Figure 4, we can observe that our proposed hybrid solution consumes less power on average than the purely acoustic or purely optical network. Compared to the related hybrid opto-acoustic technique in [23], our solution consumes much less power throughout the 6-day period.

On days 3 and 4, optical power consumption is high, causing our proposed solution to consume as much, and in some instances, even more power as compared to the purely acoustic network. It should be noted from Figure 3d that the mean optical absorption coefficients are higher on days 3 and 4, resulting in a higher target optical SNR, causing the optical power consumption to rise significantly during these two days. Accordingly, it is evident that a higher optical power component resulted in higher overall power consumption for our proposed hybrid solution in these two days. In addition, a worse channel SNR has caused the related hybrid work in [23] to consume higher power compared to the rest.

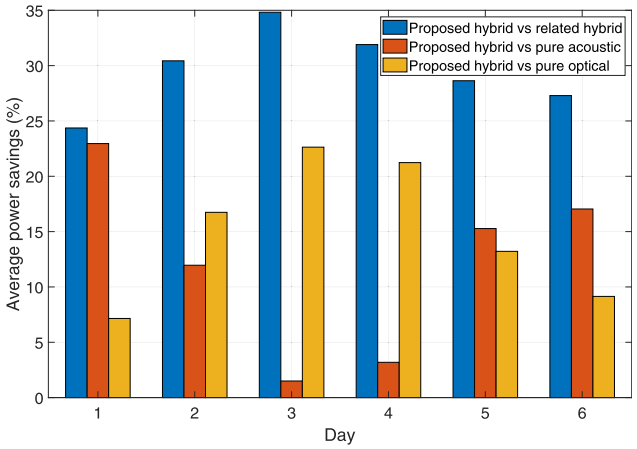

FIGURE 5. Average power savings (%) by the proposed hybrid solution compared to related hybrid [23], pure UAC and UOC over 6 days.

As discussed above, our proposed solution consumes less power on average which is evident from Figure 5. We can clearly deduce from the figure that our solution can save up to 23% power for UWCN given the dynamic nature of traffic and varying weather conditions. Although our solution may consume more power during a few hours compared to other solutions (days 3 and 4 in Figure 4), it still consumes less power on average. We can observe this in the average power savings for days 3 and 4, shown in Figure 5. On these days, our proposed hybrid technique saves 3-4% more power compared to the pure acoustic solution, but excels when compared to the pure optical network by a margin of over 20%, given adverse water/weather condition for optical links. Moreover, compared to the related hybrid work in [23], our work delivers up to 35% power savings as observed on day 3.

Furthermore, we studied the performance of our proposed solution in terms of offered and received traffic load for the period of 6 days. We compared the performance of our proposed solution to the purely acoustic, purely optical, and related hybrid opto-acoustic UWCN, and present these results in Figure 6. We observed that our hybrid solution outperforms all other solutions in terms of received traffic. The figure shows average traffic load over a period of 24 hours for each day and our proposed solution always delivers a higher traffic compared to the other three solutions.

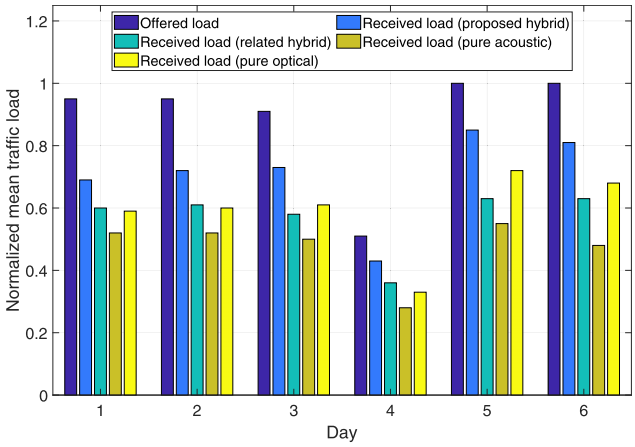

FIGURE 6. Normalized mean offered load and received load for the proposed hybrid, related hybrid [23], pure acoustic, and pure optical solutions over 6 days.

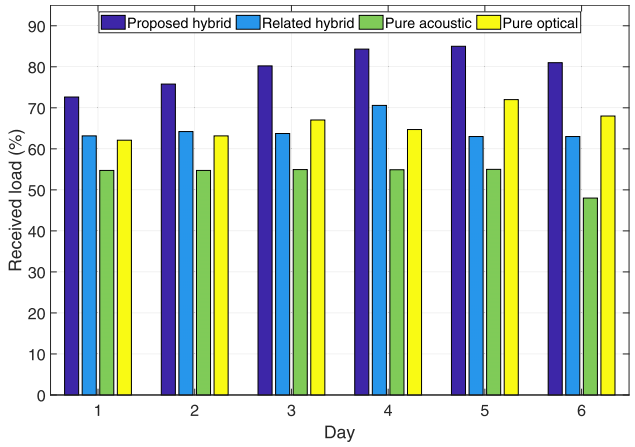

FIGURE 7. Received load (%) for the proposed hybrid, related hybrid [23], pure acoustic, and pure optical solutions over 6 days.

Additionally, a comparison of the ratio of received and offered load for the proposed hybrid, related hybrid, pure acoustic, and pure optical solutions is presented in Figure 7. The figure substantiates that our proposed solution delivers more than 70% of the offered load throughout the period of 6 days, outperforming all other solutions. The pure optical solution can deliver 70% of the load only on one occasion (Day 5), whilst the pure acoustic network performs poorly with less than 60% received load compared to the offered load throughout the period of 6 days.

Moreover, our results in Figure 7 show that the related hybrid solution performs better than a pure acoustic network in terms of the percentage of received traffic load.

TABLE 3. Summary of the results obtained.

		Pure acoustic	Pure optical	Related hybrid	Proposed hybrid
Day 1	Average Power Consumption (W)	261.5	217.3	268.4	201.4
	Received Load (%)	54.7	62.1	63.1	72.6
Day 2	Average Power Consumption (W)	263.7	280.1	334.1	232.2
	Received Load (%)	54.7	63.2	64.2	75.8
Day 3	Average Power Consumption (W)	265.5	338.3	401.4	261.5
	Received Load (%)	54.9	67.3	63.7	80.2
Day 4	Average Power Consumption (W)	261.3	322.5	374.7	252.9
	Received Load (%)	54.9	64.7	70.6	84.3
Day 5	Average Power Consumption (W)	263.4	257.7	313.3	223.2
	Received Load (%)	55.0	72.0	63.0	68.1
Day 6	Average Power Consumption (W)	272.9	247.9	310.2	224.8
	Received Load (%)	48.0	68.0	63.0	81.0

Since the related hybrid solution does not implement optimization for power consumption, it consumes more power than pure acoustic and optical solutions. However, the related hybrid solution yields better performance in terms of throughput compared to pure acoustic because of the high-speed optical component of the hybrid system. When compared to our proposed solution, however, the related hybrid underperforms in terms of both power consumption and throughput, as observed in Figures 4 and 7 respectively.

All these results are summarized and presented in Table 3, indicating that our proposed hybrid opto-acoustic solution saves power and is more robust to dynamic underwater traffic and weather conditions compared to the related hybrid, standalone acoustic and optical solutions.

However, as discussed before, since the proposed optimization model belongs to the class of NP-hard problems, the computational time and complexity is expected to increase as the network size grows with more nodes and links. But because the problem can be solved offline periodically (e.g., hourly), the additional computational complexity to find the optimum solution for larger networks is not a limiting factor for practical applications. Moreover, heuristic-based suboptimal solutions with lower computational complexities can be utilized to reduce power consumption in larger networks. In our future works, we intend to explore such heuristic-based solutions.

VII. CONCLUSION

In this paper, we have proposed a hybrid opto-acoustic UWC technique that saves power without compromising network throughput. Our technique delivers low power consumption solutions that consider the dynamic nature of underwater conditions and varying traffic loads. Our solution utilizes the two most common UWC PHY-layer technologies, underwater acoustics and optics, and combines them so that their strengths and weaknesses complement each other to deliver a reliable UWCN that also saves power. When changing weather conditions and traffic demands are unsuitable for acoustics, our system switches to optical and vice versa. Under some circumstances, both of these technologies operate in conjunction to satisfy the traffic demand while also saving power. Our proposed strategy can save power by up to 23% compared to the standalone acoustic or optical solutions. Moreover, it can deliver up to 35% power-savings compared to a related hybrid opto-acoustic solution proposed in the literature. This power-saving technique is expected to act as a significant driver for green underwater communication, paving the pathway for a green IoUT.

APPENDIX A
BREAKDOWN OF THE ACOUSTIC ABSORPTION COEFFICIENT FORMULA

In the first term of equation (4), A_1 is the boric acid component, P_1 is the depth pressure resulting from A_1, f_1 is the relaxation frequency for the boric acid component in seawater and are given respectively as

$$A_1 = \frac{8.68}{c} \times 10^{(0.78pH-5)} \tag{45}$$

$$P_1 = 1 \tag{46}$$

$$f_1 = 2.8\sqrt{\frac{S}{35}} \times 10^{(4-1245/273+T)} \tag{47}$$

where c is the underwater sound speed (m/s), pH is the water pH, S is salinity (parts per thousand (PPT)), and T is temperature (°C).

In the second term, A_2 is the magnesium sulfate component, P_1 is the depth pressure resulting from A_2, and f_2 is the relaxation frequency for the magnesium sulfate component in seawater. They can be expressed respectively as

$$A_2 = 21.44\left(\frac{S}{c}\right) \times (1 + 0.025T) \tag{48}$$

$$P_2 = 1 - 1.37 \times 10^{-4} z + 6.2 \times 10^{-9} z^2 \quad (49)$$

$$f_2 = \frac{8.17 \times 10^{(8-1990/273+T)}}{1 + 0.0018(S-35)} \quad (50)$$

where z is the water depth.

Lastly, in the third term, A_3 is the pure water viscosity component (dB km $^{-1}$ kHz^2), and P_3 is the depth pressure resulting from A_3, and they are given by

$$A_3 = \begin{cases} 4.937 \times 10^{-4} - 2.59 \times 10^{-5} T \\ + 9.11 \times 10^{-7} T^2 - 1.5 \times 10^{-8} T^3, \\ \text{for } T \leq 20°\text{C}, \end{cases} \quad (51a)$$

$$\begin{cases} 3.964 \times 10^{-4} - 1.146 \times 10^{-5} T \\ + 1.45 \times 10^{-7} T^2 - 6.65 \times 10^{-10} T^3, \\ \text{for } T > 20°\text{C}. \end{cases} \quad (51b)$$

$$P_3 = 1 - 3.83 \times 10^{-5} z + 4.9 \times 10^{-10} z^2 \quad (52)$$

REFERENCES

[1] Z. Zeng, S. Fu, H. Zhang, Y. Dong, and J. Cheng, "A survey of underwater optical wireless communications," *IEEE Commun. Surveys Tuts.*, vol. 19, no. 1, pp. 204–238, 1st Quart., 2017.

[2] H. Kaushal and G. Kaddoum, "Underwater optical wireless communication," *IEEE Access*, vol. 4, pp. 1518–1547, 2016.

[3] I. I. Smolyaninov, Q. Balzano, C. C. Davis, and D. Young, "Surface wave based underwater radio communication," *IEEE Antennas Wireless Propag. Lett.*, vol. 17, no. 12, pp. 2503–2507, Dec. 2018.

[4] L. Liu, M. Ma, C. Liu, and Y. Shu, "Optimal relay node placement and flow allocation in underwater acoustic sensor networks," *IEEE Trans. Commun.*, vol. 65, no. 5, pp. 2141–2152, May 2017.

[5] D. B. Kilfoyle and A. B. Baggeroer, "The state of the art in underwater acoustic telemetry," *IEEE J. Ocean. Eng.*, vol. 25, no. 1, pp. 4–27, Jan. 2000.

[6] E. M. Sozer, M. Stojanovic, and J. G. Proakis, "Underwater acoustic networks," *IEEE J. Ocean. Eng.*, vol. 25, no. 1, pp. 72–83, Jan. 2000.

[7] Z. Ghassemlooy, S. Arnon, M. Uysal, Z. Xu, and J. Cheng, "Emerging optical wireless communications-advances and challenges," *IEEE J. Sel. Areas Commun.*, vol. 33, no. 9, pp. 1738–1749, Sep. 2015.

[8] I. F. Akyildiz, P. Wang, and Z. Sun, "Realizing underwater communication through magnetic induction," *IEEE Commun. Mag.*, vol. 53, no. 11, pp. 42–48, Nov. 2015.

[9] M. C. Domingo, "Magnetic induction for underwater wireless communication networks," *IEEE Trans. Antennas Propag.*, vol. 60, no. 6, pp. 2929–2939, Jun. 2012.

[10] M. Jouhari, K. Ibrahimi, H. Tembine, and J. Ben-Othman, "Underwater wireless sensor networks: A survey on enabling technologies, localization protocols, and Internet of underwater things," *IEEE Access*, vol. 7, pp. 96879–96899, 2019.

[11] M. C. Domingo, "An overview of the Internet of underwater things," *J. Netw. Comput. Appl.*, vol. 35, no. 6, pp. 1879–1890, 2012.

[12] J. Heidemann, W. Ye, J. Wills, A. Syed, and Y. Li, "Research challenges and applications for underwater sensor networking," in *Proc. IEEE Wireless Commun. Netw. Conf. (WCNC)*, vol. 1, Apr. 2006, pp. 228–235.

[13] S. Melman, A. Pavin, V. Bobkov, and A. Inzartsev, "Distributed simulation framework for investigation of autonomous underwater vehicles' real-time behavior," in *Proc. MTS/IEEE OCEANS*, Oct. 2015, pp. 1–8.

[14] E. Demirors, G. Sklivanitis, T. Melodia, S. N. Batalama, and D. A. Pados, "Software-defined underwater acoustic networks: Toward a high-rate real-time reconfigurable modem," *IEEE Commun. Mag.*, vol. 53, no. 11, pp. 64–71, Nov. 2015.

[15] J. A. Catipovic, "Performance limitations in underwater acoustic telemetry," *IEEE J. Ocean. Eng.*, vol. 15, no. 3, pp. 205–216, Jul. 1990.

[16] W. C. Cox, J. A. Simpson, and J. F. Muth, "Underwater optical communication using software defined radio over LED and laser based links," in *Proc. Mil. Commun. Conf. (MILCOM)*, Nov. 2011, pp. 2057–2062.

[17] B. Shihada, O. Amin, C. Bainbridge, S. Jardak, O. Alkhazragi, T. K. Ng, B. Ooi, M. Berumen, and M.-S. Alouini, "Aqua-fi: Delivering Internet underwater using wireless optical networks," *IEEE Commun. Mag.*, vol. 58, no. 5, pp. 84–89, May 2020.

[18] M. V. Jamali, F. Akhoundi, and J. A. Salehi, "Performance characterization of relay-assisted wireless optical CDMA networks in turbulent underwater channel," *IEEE Trans. Wireless Commun.*, vol. 15, no. 6, pp. 4104–4116, Jun. 2016.

[19] I. Vasilescu, K. Kotay, D. Rus, M. Dunbabin, and P. Corke, "Data collection, storage, and retrieval with an underwater sensor network," in *Proc. 3rd Int. Conf. Embedded Netw. Sensor Syst. (SenSys)*, 2005, pp. 154–165.

[20] N. Farr, A. Bowen, J. Ware, C. Pontbriand, and M. Tivey, "An integrated, underwater optical/acoustic communications system," in *Proc. IEEE OCEANS*, May 2010, pp. 1–6.

[21] T. Hu and Y. Fei, "MURAO: A multi-level routing protocol for acoustic-optical hybrid underwater wireless sensor networks," in *Proc. 9th Annu. IEEE Commun. Soc. Conf. Sensor, Mesh Ad Hoc Commun. Netw. (SECON)*, Jun. 2012, pp. 218–226.

[22] S. Han, Y. Noh, R. Liang, R. Chen, Y.-J. Cheng, and M. Gerla, "Evaluation of underwater optical-acoustic hybrid network," *China Commun.*, vol. 11, no. 5, pp. 49–59, May 2014.

[23] J. Wang, W. Shi, L. Xu, L. Zhou, Q. Niu, and J. Liu, "Design of optical-acoustic hybrid underwater wireless sensor network," *J. Netw. Comput. Appl.*, vol. 92, pp. 59–67, Aug. 2017.

[24] M. Mostafa, H. Esmaiel, and E. M. Mohamed, "A comparative study on underwater communications for enabling C/U plane splitting based hybrid UWSNs," in *Proc. IEEE Wireless Commun. Netw. Conf. (WCNC)*, Apr. 2018, pp. 1–6.

[25] B. Mukherjee and P. Chowdhury, "Green wireless-optical broadband access network (WOBAN)," in *Proc. Asia Commun. Photon. Conf. Exhib.*, 2009, pp. 1–2.

[26] J. Lorincz, T. Garma, and G. Petrovic, "Measurements and modelling of base station power consumption under real traffic loads," *Sensors*, vol. 12, no. 4, pp. 4281–4310, Mar. 2012.

[27] M. Ahmed, I. Ahmad, and D. Habibi, "Load-adaptive resource management for green wireless-optical broadband access network (WOBAN)," *J. Lightw. Technol.*, vol. 34, no. 10, pp. 2359–2370, May 15, 2016.

[28] M. M. Mowla, I. Ahmad, D. Habibi, and Q. V. Phung, "A green communication model for 5G systems," *IEEE Trans. Green Commun. Netw.*, vol. 1, no. 3, pp. 264–280, Sep. 2017.

[29] J. Heidemann, M. Stojanovic, and M. Zorzi, "Underwater sensor networks: Applications, advances and challenges," *Phil. Trans. Roy. Soc. A, Math., Phys. Eng. Sci.*, vol. 370, no. 1958, pp. 158–175, Jan. 2012.

[30] M. Doniec, A. Xu, and D. Rus, "Robust real-time underwater digital video streaming using optical communication," in *Proc. IEEE Int. Conf. Robot. Autom.*, May 2013, pp. 5117–5124.

[31] S. Han, Y. Noh, U. Lee, and M. Gerla, "Optical-acoustic hybrid network toward real-time video streaming for mobile underwater sensors," *Ad Hoc Netw.*, vol. 83, pp. 1–7, Feb. 2019.

[32] R. B. Wynn, V. A. I. Huvenne, T. P. Le Bas, B. J. Murton, D. P. Connelly, B. J. Bett, H. A. Ruhl, K. J. Morris, J. Peakall, D. R. Parsons, E. J. Sumner, S. E. Darby, R. M. Dorrell, and J. E. Hunt, "Autonomous underwater vehicles (AUVs): Their past, present and future contributions to the advancement of marine geoscience," *Mar. Geol.*, vol. 352, pp. 451–468, Jun. 2014.

[33] H. Baumann, "Temperature, pH, DO, and salinity data from Mumford Cove, Connecticut, USA from 2015–2020," Biological Chem. Oceanogr. Data Manage. Office, Univ. Connecticut, Storrs, CT, USA, Tech. Rep., 2020. [Online]. Available: https://hdl.handle.net/1912/25578, doi: 10.26008/1912/bco-dmo.659874.2.

[34] M. Medina and R. Iglesias-Prieto, "Irradiance and estimated light attenuation coefficient, Kd, underwater and onshore in Varadero Reef, 2017," Biol. Chem. Oceanogr. Data Manage. Office, Pennsylvania State Univ., State College, PA, USA, Tech. Rep., 2020. [Online]. Available: https://hdl.handle.net/1912/25476, doi: 10.1575/1912/bco-dmo.786608.1.

[35] J. Preisig, "Acoustic propagation considerations for underwater acoustic communications network development," *ACM SIGMOBILE Mobile Comput. Commun. Rev.*, vol. 11, no. 4, pp. 2–10, Oct. 2007.

[36] C. M. G. Gussen, P. S. R. Diniz, M. L. R. Campos, W. A. Martins, and J. N. Gois, "A survey of underwater wireless communication technologies," *J. Commun. Inf. Sys.*, vol. 31, no. 1, pp. 242–255, 2016.

[37] L. J. Johnson, R. J. Green, and M. S. Leeson, "Hybrid underwater optical/acoustic link design," in *Proc. 16th Int. Conf. Transparent Opt. Netw. (ICTON)*, Jul. 2014, pp. 1–4.

[38] N. Morozs, W. Gorma, B. T. Henson, L. Shen, P. D. Mitchell, and Y. V. Zakharov, "Channel modeling for underwater acoustic network simulation," *IEEE Access*, vol. 8, pp. 136151–136175, 2020.

[39] M. C. Domingo, "Overview of channel models for underwater wireless communication networks," *Phys. Commun.*, vol. 1, no. 3, pp. 163–182, Sep. 2008.
[40] R. E. Francois and G. R. Garrison, "Sound absorption based on ocean measurements: Part I: Pure water and magnesium sulfate contributions," *J. Acoust. Soc. Amer.*, vol. 72, no. 3, pp. 896–907, Sep. 1982.
[41] R. E. Francois and G. R. Garrison, "Sound absorption based on ocean measurements. Part II: Boric acid contribution and equation for total absorption," *J. Acoust. Soc. Amer.*, vol. 72, no. 6, pp. 1879–1890, Dec. 1982.
[42] M. Stojanovic, "On the relationship between capacity and distance in an underwater acoustic communication channel," in *Proc. 1st ACM Int. Workshop Underwater Netw. (WUWNet)*. New York, NY, USA: Association for Computing Machinery, 2006, pp. 41–47.
[43] B. Pranitha and L. Anjaneyulu, "Review of research trends in underwater communications—A technical survey," in *Proc. Int. Conf. Commun. Signal Process. (ICCSP)*, Apr. 2016, pp. 1443–1447.
[44] H. Esmaiel and D. Jiang, "Review article: Multicarrier communication for underwater acoustic channel," *Int. J. Commun., Netw. Syst. Sci.*, vol. 6, no. 8, p. 361, 2013.
[45] J. A. Simpson, B. L. Hughes, and J. F. Muth, "Smart transmitters and receivers for underwater free-space optical communication," *IEEE J. Sel. Areas Commun.*, vol. 30, no. 5, pp. 964–974, Jun. 2012.
[46] F. Xing, H. Yin, Z. Shen, and V. C. M. Leung, "Joint relay assignment and power allocation for multiuser multirelay networks over underwater wireless optical channels," *IEEE Internet Things J.*, vol. 7, no. 10, pp. 9688–9701, Oct. 2020.
[47] S. Jaruwatanadilok, "Underwater wireless optical communication channel modeling and performance evaluation using vector radiative transfer theory," *IEEE J. Sel. Areas Commun.*, vol. 26, no. 9, pp. 1620–1627, Dec. 2008.
[48] J. W. Giles and I. N. Bankman, "Underwater optical communications systems. Part 2: Basic design considerations," in *Proc. IEEE Mil. Commun. Conf. (MILCOM)*, vol. 3, Oct. 2005, pp. 1700–1705.
[49] M. Gao, C. H. Foh, and J. Cai, "On the selection of transmission range in underwater acoustic sensor networks," *Sensors*, vol. 12, no. 4, pp. 4715–4729, Apr. 2012.
[50] D. Anguita, D. Brizzolara, G. Parodi, and Q. Hu, "Optical wireless underwater communication for AUV: Preliminary simulation and experimental results," in *Proc. IEEE OCEANS*, Jun. 2011, pp. 1–5.
[51] P. Kovács, "Minimum-cost flow algorithms: An experimental evaluation," *Optim. Methods Softw.*, vol. 30, no. 1, pp. 94–127, Jan. 2015.
[52] M. Conforti, G. Cornuéjols, and G. Zambelli, *Integer Programming*, vol. 271. Cham, Switzerland: Springer, 2014, doi: 10.1007/978-3-319-11008-0.
[53] *ILOG CPLEX Optimization Studio User's Manual 12.8*, Armonk, New York, NY, USA, 2017.

KAZI YASIN ISLAM (Student Member, IEEE) received the B.E. degree in electrical and computer systems engineering from Monash University, Malaysia, in 2015, and the M.E. degree in electronics and communication engineering from Edith Cowan University, Australia, in 2019, where he is currently pursuing the Ph.D. degree. His research interests include underwater wireless communication, green communication, the IoT, and machine learning.

IFTEKHAR AHMAD (Member, IEEE) received the Ph.D. degree in communication networks from Monash University, Australia, in 2007. He is currently an Associate Professor with the School of Engineering, Edith Cowan University, Australia. His research interests include 5G technologies, green communications, QoS in communication networks, software-defined radio, wireless sensor networks, and computational intelligence.

DARYOUSH HABIBI (Senior Member, IEEE) received the B.E. degree (Hons.) in electrical engineering and the Ph.D. degree from the University of Tasmania, Australia, in 1989 and 1994, respectively. His employment history includes Telstra Research Laboratories, Flinders University, Intelligent Pixels, Inc., and Edith Cowan University, where he is currently a Professor, the Pro Vice-Chancellor, and the Executive Dean of Engineering. His current research interests include engineering design for sustainable development, smart energy systems, environmental monitoring technologies, and reliability and quality of service in communication systems. He is a fellow of Engineers, Australia, and the Institute of Marine Engineering, Science and Technology.

M. ISHTIAQUE A. ZAHED received the Ph.D. degree from Edith Cowan University, Australia, in 2020. He is currently an Assistant Professor with the School of Science, Engineering and Technology, East Delta University, Bangladesh. His research interests include green communications, the IoT, next generation networks, and network security.

JOARDER KAMRUZZAMAN (Senior Member, IEEE) is currently a Professor with the School of Engineering, IT and Physical Sciences, Federation University. He has published over 250 peer-reviewed publications. His interests include the Internet of Things, machine learning, and cybersecurity. He has received nearly A$2.4m research funding, including prestigious ARC and large collaborative research center grants. He is an Editor of the *Journal of Network and Computer Applications* (Elsevier).